Nonlinear degradation of O-X-B mode conversion in MAST Upgrade

Mads Givskov Senstius[1,*], *Simon James* Freethy[2], and *Stefan Kragh* Nielsen[1]

[1]Department of Physics, Technical University of Denmark, Fysikvej, DK-2800 Kgs. Lyngby, Denmark
[2]Culham Centre for Fusion Energy, UKAEA, Abingdon, OX14 3DB, United Kingdom

Abstract. Spherical tokamaks like the MAST Upgrade device are often operated in an overdense regime. As a consequence, conventional electron cyclotron resonance heating (ECRH) and current drive (ECCD) are typically not possible. MAST Upgrade is planned to investigate a mode coupling scheme known as O-X-B at high power, which may allow gyrotrons to heat and drive current in overdense plasmas by coupling electromagnetic waves to electrostatic electron Bernstein waves (EBWs) at the upper hybrid (UH) layer. However at the gyrotron beam intensities planned for MAST Upgrade, several nonlinear effects may degrade the linear mode coupling into EBWs. Using particle-in-cell simulations, parametric decay instabilities (PDIs) and stochastic electron heating (SEH) are investigated in the region near the UH layer. It is found that nonlinear effect could have a substantial impact on the O-X-B scheme in MAST Upgrade at high gyrotron intensities.

1 Introduction

Spherical tokamaks are often operated in a highly overdense regime, which means that their core is unavailable to electron cyclotron (EC) resonance heating (ECRH) and current drive (ECCD) at several of the lowest harmonics. However, a mode coupling scheme known as O-X-B[1] may enable the use of high power microwaves for heating and current drive in such plasmas. The O-X-B scheme couples electromagnetic waves from e.g. a gyrotron to electrostatic waves known as electron Bernstein waves (EBWs)[2] which can propagate without a high density cutoff and are strongly damped at the electron cyclotron resonances. The use of EBWs is considered a key enabling technology at MAST Upgrade which has acquired two 28/34.8 GHz gyrotrons chosen specifically for O-X-B instead of regular ECCD. Although the mode coupling scheme is promising at low power densities[3], a number of nonlinear effects may degrade its performance when unprecedented gyrotron power levels are used for O-X-B operation. Parametric decay instabilities (PDIs) and stochastic electron heating (SEH) are considered likely nonlinear loss mechanisms in upcoming MAST Upgrade EBW experiments. Even though the conversion rate of O-X-B is favorable at low power, it may scale unfavorably with an increase in power above a nonlinear threshold. The follow up device to MAST Upgrade will be the prototype fusion power plant STEP which is to be a microwave driven machine. If the promising low power O-X-B results remain at higher gyrotron power levels, STEP may employ O-X-B as its main current drive scheme.

The EBWs are excited at the upper hybrid (UH) layer where PDIs are known to take place even at comparably low power densities. PDIs are unstable nonlinear wave interactions which may cause power to be diverted away from the gyrotron beam into waves at undesired frequencies. In addition to the PDIs, EBWs can also experience strong damping due to SEH. The EBWs are carried by gyrating electrons but the electron gyromotion gets warped if the EBW amplitude is too large. Instead of an energy conserving orbit, the electrons may then follow stochastic trajectories with periods of substantial acceleration. Both nonlinear effects could lead to great losses in the outer parts of the plasma.

In this contribution, we investigate the frequencies that are likely to be excited in PDIs during O-X-B in MAST Upgrade as well as a threshold for SEH to set in. We compare with particle-in-cell simulations and look at the power scaling of O-X-B. Although both PDIs and SEH can be considered loss mechanisms, they have different impacts on how a gyrotron beam interacts with a plasma. We discuss how both impact mode coupling schemes involving EBWs.

2 Theory

2.1 The O-X-B mode coupling scheme

For the conventional microwave based heating and current drive schemes, a high power microwave source injects an electromagnetic wave, typically O- or X-mode, into the plasma and is absorbed at a low EC harmonic near the core of the plasma. In overdense plasmas such as the MAST Upgrade and other spherical tokamaks, the electron cyclotron frequency is small compared to the plasma frequency and the confined core becomes unavailable to O- and X-mode. However by angling an O-mode beam optimally to the magnetic field, it can couple to slow X-mode at the plasma frequency inside the plasma, which in

*e-mail: mgse@fysik.dtu.dk

turn can couple to an electrostatic EBW at the UH layer[1]. Figure 1a shows an O-X-B trajectory calculated with a ray tracer, dividing it into segments associated with the O-, X- and EBW. Where exactly the X-mode ends and the EBW start is debatable as the transition is smooth. Near the UH layer, X-mode becomes longitudinal and the wave characteristics become similar to that EBWs under an electrostatic approximation, but we instead define the forward propagating wave as X-mode, the backward propagating wave as the EBW and the turning point as the UH layer. For typical MAST Upgrade parameters, this occurs between the 2nd and 3rd EC resonances and the turning point is then outside the UH frequency layer as can be seen in figure 1a.

This mode coupling scheme is called O-X-B and can be utilized to get microwave radiation absorbed at the core of an overdense plasma as EBWs can propagate without a high density cutoff. At low power, the O-X-B scheme has shown to drive current more efficiently than conventional ECCD. However, the UH layer where X is coupled to EBW is a resonant region where nonlinear effect can become significant. The impact of nonlinear effects on O-X-B is not well known at the high gyrotron beam intensities that the MAST Upgrade gyrotron system will be capable of delivering to the UH layer.

2.2 Parametric decay instabilities (PDIs)

One of the nonlinearities commonly associated with the mode coupling at the UH layer is three-wave interactions. One of the most well documented three-wave interaction for X to EBW conversion is a decay event where the X-mode gyrotron pump wave excites an EBW and a lower hybrid (LH) wave[2]. The process conserves frequency and wave vector which leads to the following selection rules

$$\omega_0 = \omega_1 + \omega_2, \quad \mathbf{k}_0 = \mathbf{k}_1 + \mathbf{k}_2, \tag{1}$$

where ω_i is the angular frequency of wave i, $\mathbf{k}_i$ its wave vector, and index 0 refers to the pump wave, while 1 and 2 refer to the daughter waves produced in the decay process. Because of the conservation of frequency, the EBW daughter wave will be produced at frequency downshifted from the pump by that of the LH daughter wave, which would be approximately the LH frequency for an interaction between these waves. The strength of the interaction between the waves depends on the amplitude of the pump wave. If the interaction is weak, damping from collisions and other effects may prevent the daughter waves from growing beyond their background level. However above a pump wave amplitude threshold, growth due to the three-wave interactions exceed the losses and the interactions manifest themselves as a parametric decay instability (PDI)[4–7]. Using [8], the threshold is $\approx 2 \times 10^5\,\mathrm{W/m^2}$ for the L-mode parameters presented later in section 3. It is also possible for three waves to interact in a combination event where typically a large amplitude pump wave combines with a natural wave of the plasma to produce a third one. Again, this process requires conservation of frequency and wave vector. Often, both decay and combination events occur in a system, producing side bands to the pump frequency, shifted by a characteristic frequency such as the LH frequency around it. The region around the UH layer is associated with PDIs because the pump wave encounters a turning point, causing its group velocity to decrease and consequently its amplitude to swell[9] in order for the flow of power to be conserved. The PDIs may be of concern because they allow for the flow of power to change characteristics. If a gyrotron beam is intended to be absorbed at a target EC resonance in the center of the plasma, a PDI may cause a substantial fraction of the power to go into waves which resonate in other parts of the plasma and propagate in entirely different directions. What is more, low power experiments do not necessarily reflect high power experiments due to the nonlinear dependence on pump wave amplitude. Upcoming O-X-B experiments at MAST Upgrade will also investigate PDIs and a radiometer is being developed to allow for signatures of nonlinear wave interactions with the gyrotron beam to be observed[10].

2.3 Stochastic electron heating (SEH)

The EBWs are longitudinal waves which propagate as coherent electron density perturbations. As the electrons gyrate around the magnetic field lines in and out of phase, they can carry an electric field which points in the same direction as it propagates. At low electric field amplitudes, the electrons are not particularly affected by the electric field of the EBW, but above a wave amplitude threshold, the electron trajectories transition from harmonic orbits around the magnetic field line into a seemingly stochastic motion. This is illustrated in figure 1b where a simple Boris solver[11] is used to calculate particle trajectories in the presence of a magnetic field and an EBW at different electric field amplitudes. Whilst the green line appears unaffected by the EBW, the orange line displays visible modifications to the radius of gyration and the blue line appears stochastic. In the stochastic regime, the electrons experience a strong acceleration and their kinetic energy can rapidly increase as they ride the waves in the electric field at the expense of the power carried by the EBW. For this reason, the term stochastic electron heating (SEH) is often used. In the literature, different conditions have been suggested for the SEH threshold[12–15]. Following [16], we introduce the normalized quantity

$$A \equiv -\frac{m_e}{eB^2}\partial_x E_x, \tag{2}$$

where m_e is the electron mass, e is the elementary charge, B is the magnitude of the background magnetic field and E_x is the electric field of a longitudinal wave propagating in the x-direction. The threshold condition for SEH is then $|A| \geq 1$ and this should lead to strong increases in electron temperature. The derivation of this expression is based on the assumption that only one wave is present but near the UH layer, both a large amplitude X- and EBW are present at the same frequency but propagating in different directions with quickly varying wave vectors and amplitudes. This makes the $\partial_x E$ tedious to calculate analytically but is easy to evaluate numerically based on data from full

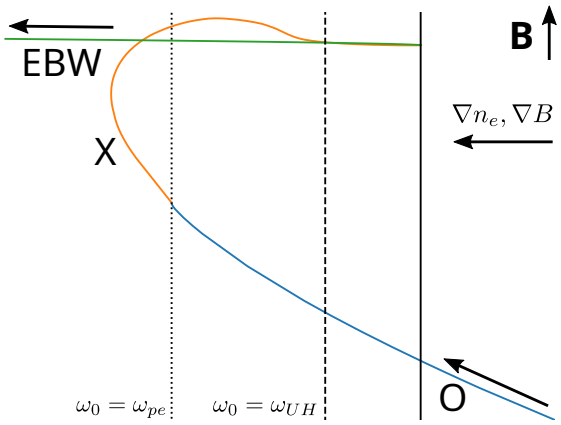

(a) Illustration of the O-X-B mode coupling scheme using a ray tracer and parameters relevant to MAST Upgrade. The injected O-mode (blue) is coupled to X-mode (orange) at the plasma frequency (dotted) by angling it correctly. X-mode then couples an EBW (green) near the UH frequency (dashed), in our definition at the turning point (solid black).

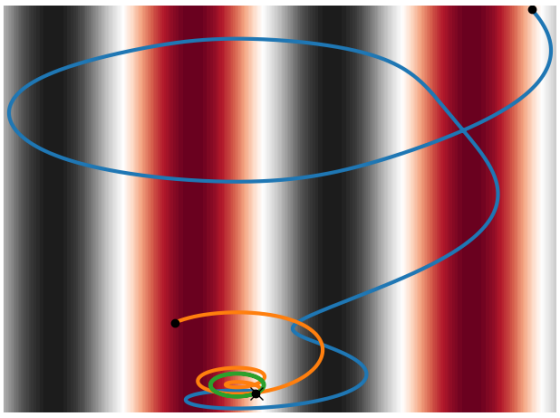

(b) Examples of electron trajectories at different EBW electric field amplitudes, an instance of the wave field is shown in the red-black heat map. The lines are for $|A| \ll 1$ (green), $|A| \approx 1$ (orange) and $|A| \gg 1$ (blue). The cross marks the starting position and circles are ending positions after 2 cyclotron periods. Trajectories are calculated using a Boris update scheme.

Figure 1: Figures illustrating basic concepts of the theory section.

wave simulations. Both the presence of two large amplitude waves as well as wave swelling near the turning point makes the UH layer a region where SEH is more likely to occur.

3 Simulations

3.1 Domain parameters

We study the impact of PDIs and SEH on O-X-B numerically using the fully kinetic particle-in-cell (PIC) code EPOCH[17, 18], focusing on the X- to EBW conversion in the vicinity of the UH layer. Whilst the conversion is a three dimensional problem, we here simplify the geometry to 1D as a first look into the problem for MAST Upgrade parameters. The gyrotron pump wave is mainly longitudinal near the UH layer and propagates close to perpendicular to the magnetic field and parallel to the direction of the density and temperature gradients. Making the 1D approximation does not affect the trajectory of the pump wave much nor should it affect SEH if the inhomogeneous direction is chosen to be perpendicular to the magnetic field. However, the small wave number component parallel to the magnetic field does lead to damping, in particular of EBWs. This may suppress some PDIs but PDIs may still excite EBWs that propagate perpendicularly to the magnetic field. In the 1D geometry, we also neglect the transverse beam profile and assume a uniform field in the homogeneous directions. In an experimental situation, the pump wave would likely have a Gaussian profile with a strong field at the center, which decreases away from the center. Gyrating and drifting particles therefore do not experience the strongest field everywhere along their trajectory. In particular, electrons spend a limited amount of time in the interaction region as they propagate across the beam profile due to their parallel velocity, and the assumption of a uniform transverse profile may therefore lead to a lower threshold[19]. We note that the electron Larmor radius is much smaller than the focused gyrotron beam at the UH layer.

The 1D approximation in terms of the EPOCH code means simply that there is only one inhomogeneous spatial direction. Macroparticles have three velocity components, which are affected by forces as expected, but only one position component. The full 6D phase space is realized by constructing 1D position space along with 3D velocity space from the macroparticles and then assuming perfect translational symmetry in the remaining position dimensions. This allow for particle orbits and drifts to be modeled even in 1D.

The code EPOCH allows for particle species to be made immobile by taking them out of the particle pusher step of the update scheme. This way, they still contribute to the background but cannot generate waves. This will be utilized to test if certain spectral features later can be explained as the result of PDIs involving ion waves.

The parameters to be investigated in this papers correspond to a high density L-mode plasma in MAST Upgrade. For a 37 GHz gyrotron beam, the region of focus between the UH layer and the L-cutoff is on the order of a centimeter long and gradients are approximately constant throughout. The UH layer is found in the pedestal, between the second and third EC resonances. The domain size is chosen to be $0.0\,\text{mm} < x < 7.5\,\text{mm}$ with $N_{\text{grid}} = 750$ grid points and $N_{\text{part}}/N_{\text{grid}} = 2000$ superparticles per grid point. The initial density and temperature are chosen to be linear profiles satisfying $n_e(0\,\text{mm}) = 2.16\times10^{19}\,\text{m}^{-3}$, $n_e(7.5\,\text{mm}) = 1.41\times10^{19}\,\text{m}^{-3}$, $T_e(0\,\text{mm}) = 63\,\text{eV}$, and

$T_e(7.5\,\mathrm{mm}) = 48\,\mathrm{eV}$. The initial ion temperature is $T_i(x) = T_e$, the magnetic field is $B = 0.46\,\mathrm{T}$ and an $\omega_0/(2\pi) = 37\,\mathrm{GHz}$ is injected at the $x = 0\,\mathrm{mm}$ in X-mode polarization. The particle boundary conditions replace escaping particles with thermally distributed particles entering the domain. The X-mode pump wave is excited at the left boundary at intensities ranging from $10^3\,\mathrm{W/m^2}$, near the background level where nonlinear effects are of little importance, up to $10^9\,\mathrm{W/m^2}$, which is the theoretical upper limit that the new MAST Upgrade gyrotron system will be able to generate.

3.2 Spectral development

As the pump wave intensity is increased from the background level, the longitudinal electric field spectrum near the pump wave develops. Before discussing nonlinear spectral features, a linear regime is established. Figure 2a shows the spectra for two low intensity simulations in the linear regime. The spectra are very similar with the main difference being the magnitude of the $\omega_0/(2\pi) = 37\,\mathrm{GHz}$ pump wave peak which increases by approximately one order of magnitude as expected.

As the pump wave intensity is increased to $I_0 = 10^5\,\mathrm{W/m^2}$, the spectrum begins to develop more broadly. Figure 2b shows the spectrum from two simulations, one where the ions have been made immobile (orange) and a regular simulation with mobile ions (blue). When ions are immobile, they provide a charge background but are taken out of the particle pusher and ion waves therefore cannot be excited. Comparing the spectra, there is a development of the spectrum around 37.25 GHz when ions are mobile. Furthermore, there is some development close to the pump frequency and figure 2c shows a zoomed spectrum near the pump. Here, symmetric sidebands shifted by ~ 20 MHz, or a few ion cyclotron frequencies, around the pump frequency has appeared when ions are mobile only, suggesting this could be the result of PDIs involving low IBW branches.

At even higher pump intensities in figure 2d, the spectrum starts to develop also at frequency shifts of approximately 0.2 GHz, which is close to the LH frequency. Two prominent symmetric peaks can be seen in the figure, only when ions are mobile, suggesting that they are the result of PDIs involving LH waves.

3.3 Indications of SEH

Around pump intensities of $10^7 - 10^8\,\mathrm{W/m^2}$, the injected pump wave reaches a magnitude where the normalized parameter A exceeds the SEH threshold $|A| \gtrsim 1$. The plots in figure 3 compare the parameter $|A|$ in the top row and the electron temperature in the bottom row. The electron temperature is calculated through the second moment of the distribution function which need not be Maxwellian. For $I_0 = 10^7\,\mathrm{W/m^2}$, the threshold is not exceeded and although a wave pattern is visible in the electron temperature, no noticeable heating is observed in particular at $x \approx 6$ mm which is near the UH layer. For $I_0 = 10^8\,\mathrm{W/m^2}$, the threshold is exceeded and a substantial heating occurs, which continues beyond the 12 ns shown in the plots. Now, the electron heating could be caused by some other process, e.g. hot electrons generated through PDIs, but the onset of rapid heating appears to agree with the SEH threshold and not the onset of PDIs which happens at much lower intensities. As the UH layer is found in the pedestal region of the MAST Upgrade plasma, SEH appears to constitute an unfavorable loss mechanism which may prevent the power of an injected beam from reaching the core of the plasma.

3.4 Impact on the linear conversion

With indications of both PDIs as well as SEH, the obvious question is how it affects the linear X- to EBW conversion. To investigate this, we use an FFT on the intervals $0.5\,\mathrm{mm} < x < 2.5\,\mathrm{mm}$ and $10\,\mathrm{ns} < t < 260\,\mathrm{ns}$ to get a spectrum in (k, ω)-space. We then identify and integrate the peaks associated with the incoming X-mode and with the returning EBW at the same frequency and sign of k. We refer to this EBW as the linearly converted EBW as we expect that it mostly comes from linear coupling with the X-mode pump at the UH layer. We do this for different pump intensities, normalize to the lowest intensity simulation and show the results in figure 4. As a sanity check, the injected X-mode pump is seen to scale close to linearly with pump intensity as expected. The returning EBW, on the other hand, scales linearly at low pump intensity but stalls around $I_0 = 10^5\,\mathrm{W/m^2}$ which is also around the point where indications of PDIs were observed in figures 2b-2c and similar to the PDI threshold predicted using [8], although this was for interactions involving LH waves. However, this particular PDI alone may not be the sole cause for the unfavorable intensity scaling. We note that there is an actual dip in conversion around where the SEH sets in, but it cannot be clearly attributed to pump losses due to SEH. Other spectral features outside the LH range also appear and may account for some of the lost pump power. These features will be the focus of later investigations. The figure predicts poor scaling of the O-X-B conversion efficiency in the intensity range that the MAST Upgrade is expected to be able to operate at, however, heating and current drive of the plasma may still occur if PDIs simply excite waves at shifted frequencies, which also propagate inwards.

Lastly, changing parameters such as pump frequency and magnetic field profile can have profound impact on the spectral development and the extend of the linear regime. Still, the theoretical upper operational limit of $I_0 = 10^9\ \mathrm{W/m^2}$ is in the nonlinear regime in all simulations so far. Even if a parallel component of the wave vector in higher dimensions may help suppress PDIs, SEH should not be affected much by this.

4 Conclusion

First considerations of nonlinear losses in connection to O-X-B operation in MAST Upgrade were presented. The

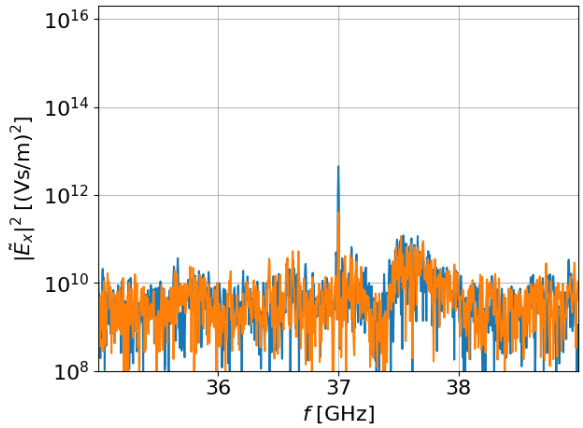

(a) Two spectra in the linear pump intensity regime. The orange line is for $I_0 = 10^3\,\mathrm{W/m^2}$ and the blue line is for $I_0 = 10^4\,\mathrm{W/m^2}$. Ions are mobile in both.

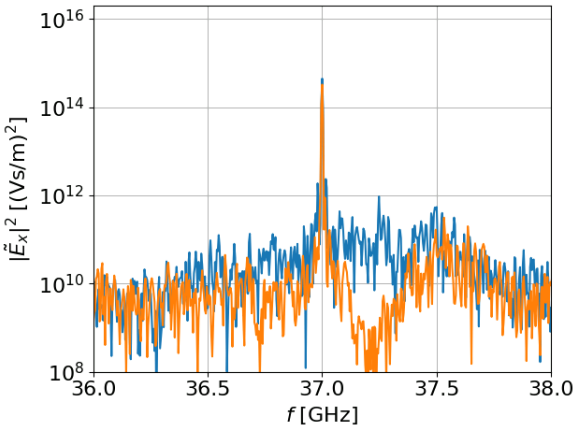

(b) The pump wave intensity is $I_0 = 10^5\,\mathrm{W/m^2}$, the orange line is for immobile ions and the blue line is for mobile ions. Notice the difference near 37.25 GHz and near the pump, see the zoom in figure 2c.

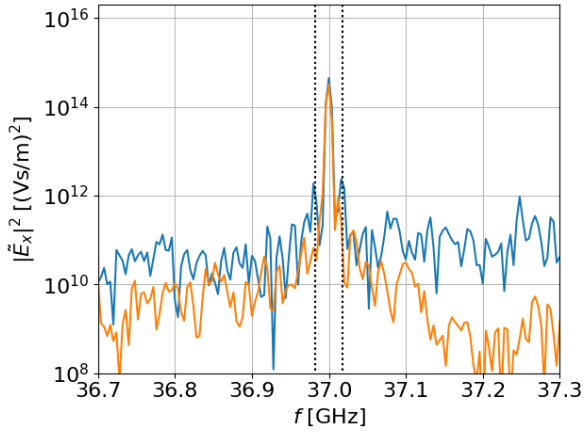

(c) Same as figure 2b but zoomed in near the pump frequency. Notice the symmetric peaks shifted by ~ 20 MHz, marked by vertical dotted lines and visible only when ions are mobile.

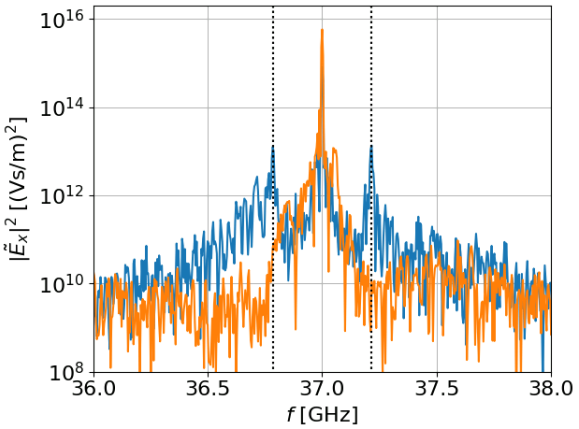

(d) The pump wave intensity is $I_0 = 10^7\,\mathrm{W/m^2}$. The orange line is for immobile ions and the blue line is for mobile ions. Notice the development ~ 0.2 GHz from the pump when the ions are mobile.

Figure 2: Frequency spectra of the longitudinal electric field spectrum near the $\omega_0/(2\pi) = 37\,\mathrm{GHz}$ pump wave.

region around the UH layer is of particular concern for both nonlinear wave interactions as well as SEH in the X- to EBW mode coupling step. PIC simulations in a simplified 1D geometry at various pump wave intensities within the operational limits of the MAST Upgrade gyrotrons show indications of both PDIs and SEH. Although a regime exists where the coupling into an EBW scales linearly with pump intensity, a fairly low intensity threshold for sublinear scaling is found around $I_0 = 10^5\,\mathrm{W/m^2}$. Whilst this first look into nonlinear degradation of O-X-B in MAST Upgrade is limited and may underestimate nonlinear thresholds due to the 1D approximation, it does justify a more thorough investigation. In particular, there were indications of spectral features outside the LH range from the pump wave which will be investigated in the future.

5 Acknowledgments

This work has been supported by research grant 15483 from VILLUM FONDEN, as well as the Enabling Reseach grant ENR-MFE19.DTU-03 and the EUROfusion Researcher Grant AWP22-ERG-DTU/Senstius from the EUROfusion Consortium. This work has been carried out within the framework of the EUROfusion Consortium, funded by the European Union via the Euratom Research and Training Programme (Grant Agreement No 101052200 — EUROfusion). Views and opinions expressed are however those of the author(s) only and do not necessarily reflect those of the European Union or the European Commission. Neither the European Union nor the European Commission can be held responsible for them. The EPOCH code used in this work was in part funded by the UK EPSRC grants EP/G054950/1, EP/G056803/1, EP/G055165/1, EP/ M022463/1 and EP/P02212X/1.

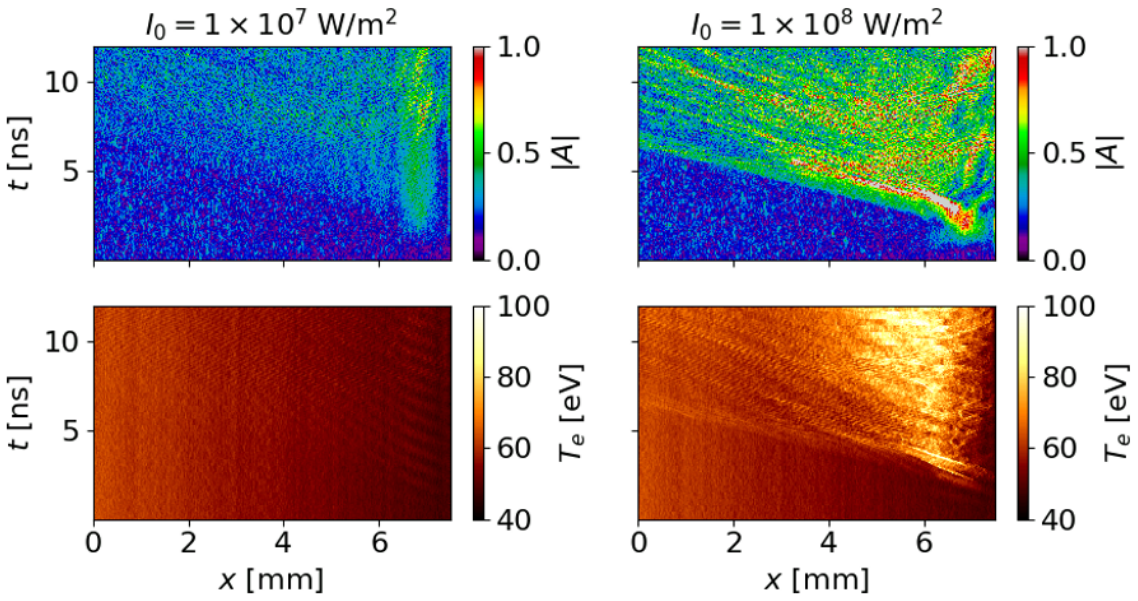

Figure 3: Comparisons of the normalized SEH parameter $|A|$ (top row) and the electron temperature (bottom row) for pump intensities around the SEH threshold of $|A| \approx 1$. The left column is below the threshold while the right column is above it.

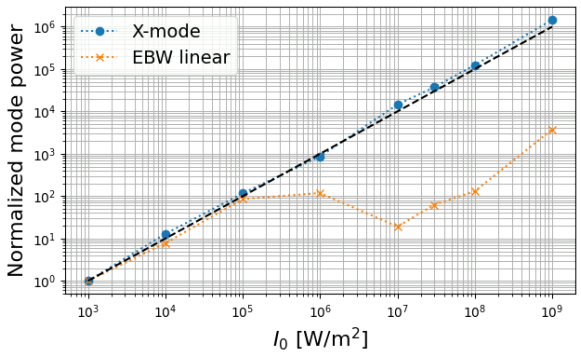

Figure 4: Scaling of X- and linearly converted EBW power with pump intensity. The points are normalized to that of the lowest intensity simulation and the dashed black line is a linear reference line.

References

[1] J. Preinhaelter and V. Kopecký, *J. Plasma Physics*, **10**, 1–12 1973.

[2] H. P. Laqua, *Plasma Physics and Controlled Fusion* **49** R01 2007

[3] V. Shevchenko, G. Cunningham, A. Gurchenko, E. Gusakov, B. Lloyd, M. O'Brien, A. Saveliev, A. Surkov, F. Volpe, and M. Walsh. *Fusion Science and Technology*, 52:2, 202–215, 2007.

[4] A.D. Piliya. Decay instability in weakly inhomogeneous plasma. *Proc. 10th Int. Conf. Phenomena in Ionized Gases (Oxford) ed Franklin R.N. (Oxford: Donald Parsons & Co. Ltd.)*, page 320, 1971.

[5] M.N. Rosenbluth. Parametric instabilities in inhomogeneous media. *Phys. Rev. Lett.*, 29:565–7, 1972.

[6] A.D. Piliya. Nonstationary theory of decay instability in a weakly inhomogeneous plasma. *Sov. Phys.–JETP*, 37:629–32, 1973.

[7] M. Porkolab and B. I. Cohen, *Nuclear Fusion*, **28**, 239, 1988.

[8] E. Z. Gusakov and A. V. Surkov, *Plasma Physics and Controlled Fusion*, **49**, 631-639, 2007

[9] R. B. White and F. F. Chen, *Plasma Physics* **16** 565–587, 1974

[10] M. G. Senstius, S. J. Freethy, J. Allen and S. K. Nielsen, *Review of Scientific Instruments* **93** 103522, 2022

[11] J. P. Boris, *Proceedings of 4th Conference on Numerical Simulation of Plasmas (Naval Research Laboratory, Washington D. C., 1970)*, pp. 3–67.

[12] J. M. McChesney, R. A. Stern and P. M. Bellan, *Physical Review Letters* **59** 1436, 1987

[13] M. Balikhin and M. Gedalin, *Physical Review Letters* **700**, 9, 1993

[14] K. Stasiewicz, R. Lundin and G. Marklund, *Physica Scripta* **T84**, 60–63, 2000

[15] C. F. F. Karney and A. Bers, *Pysical Review Letters* **39**, 9, 1977

[16] D. C. Speirs, B. Eliasson and L. K. S. Daldorff, *Journal Geophysics Research Space Physics*, **122**, 10,638–10,650, 2017

[17] T. D. Arber *et al*, *Plasma Physics and Controlled Fusion*, **57**, 113001, 2015

[18] M. G. Senstius, S. K. Nielsen, R. G. Vann and S. K. Hansen, *Plasma Physics and Controlled Fusion*, **62**, 025010, 2020

[19] R. Kamendje, S. V. Kasilov, W. Kernbichler, I. V. Pavlenko, E. Poli and M. F. Heyn, *Physics of Plasmas*, **12**, 012502, 2005